

Supporting Information

Nucleation Ability of Thermally Reduced Graphene Oxide for Polylactide: Role of Size and Structural Integrity

Yuan-Ying Liang, Su Yang, Xin Jiang, Gan-Ji Zhong,

Jia-Zhuang Xu,^{*} and Zhong-Ming Li^{*}

College of Polymer Science and Engineering, State Key Laboratory of Polymer
Materials Engineering, Sichuan University, Chengdu, 610065, People's Republic of
China

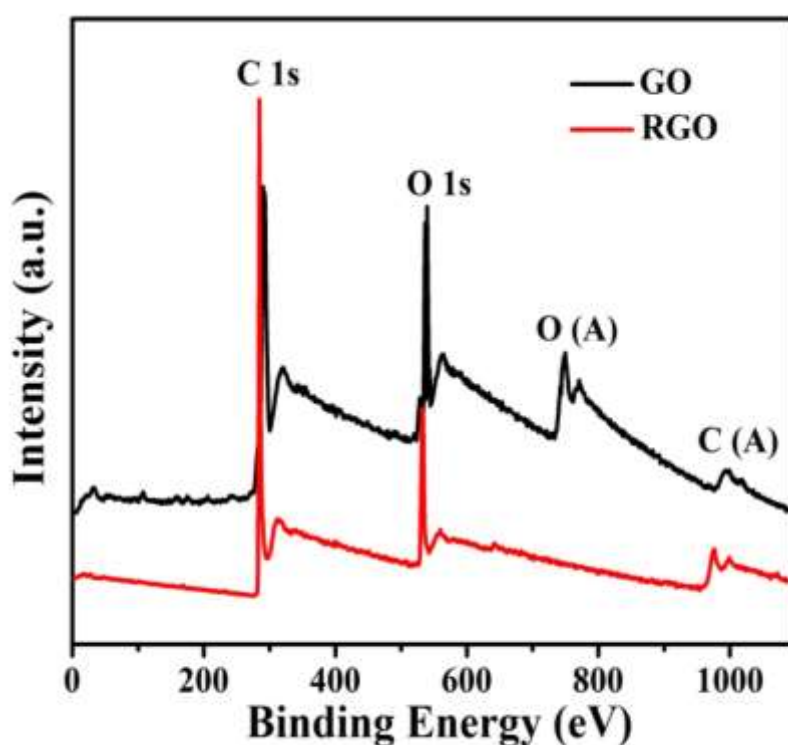


Figure S1. XPS survey scans of GO and RGO.

^{*}E-mail: zmli@scu.edu.cn; jzxu@scu.edu.cn

X-ray photoelectron (XPS) spectra were recorded on an ESCA LAB 250 spectrometer (VG Scientific) with an Al K α radiation (1486.6 eV) to characterize the surface composition of GO and RGO. As depicted in Figure S1, the C/O atomic ratio of GO and RGO is 3.0 and 13.2, respectively, manifesting that most of oxygen-containing groups were removed by thermal reduction at 900 °C.

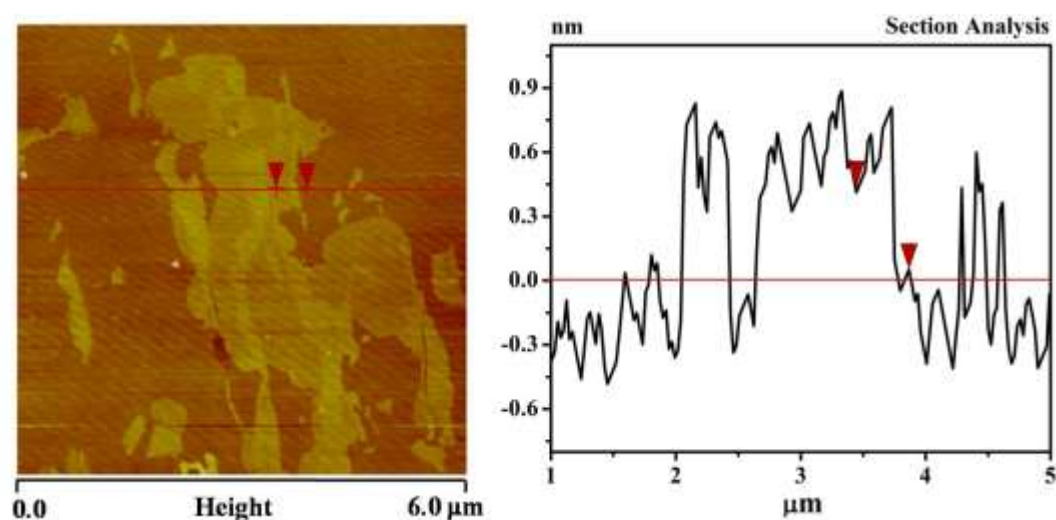
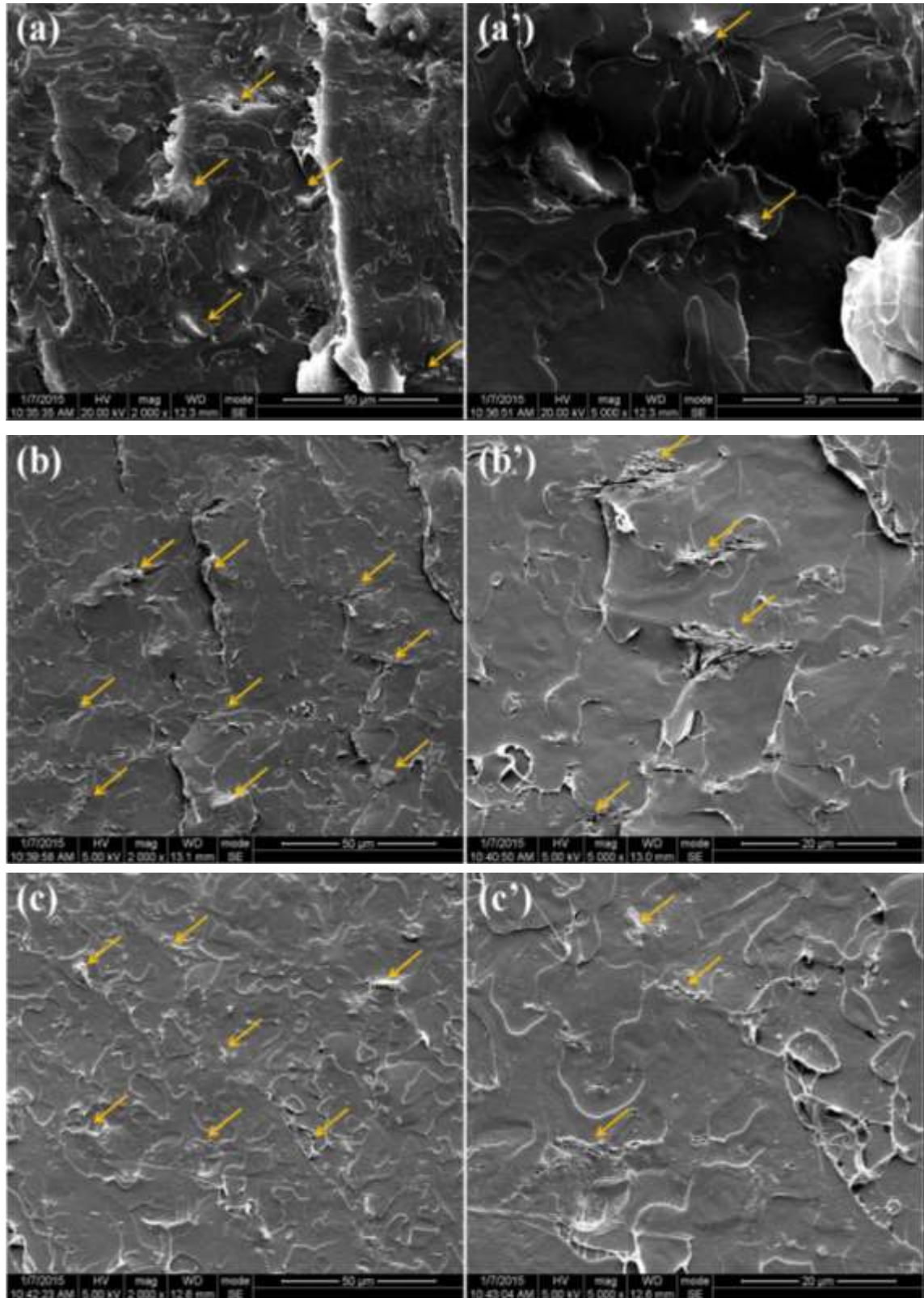


Figure S2. AFM image of RGOw0.5.

Thickness of RGO was examined by a Nanoscope Multimode & Explore atomic force microscope (AFM) (Veeco Instruments, USA) with a line scan rate of 2 Hz and line scanning of 256 under ambient conditions. Samples for AFM observation were prepared by depositing dispersions of RGO in the solution of ethanol on a fresh mica substrate and allowing them to dry in a vacuum oven before test. Typical tapping-mode AFM image and the corresponding height profile of RGOw0.5 are shown in Figure S2. From the height analysis, single RGO with an average thickness of 1 nm is visualized, which is comparable to the theoretical thickness of a

single-layer graphene.¹ The AFM characterization confirms a single-layer structure of RGO used in this work.



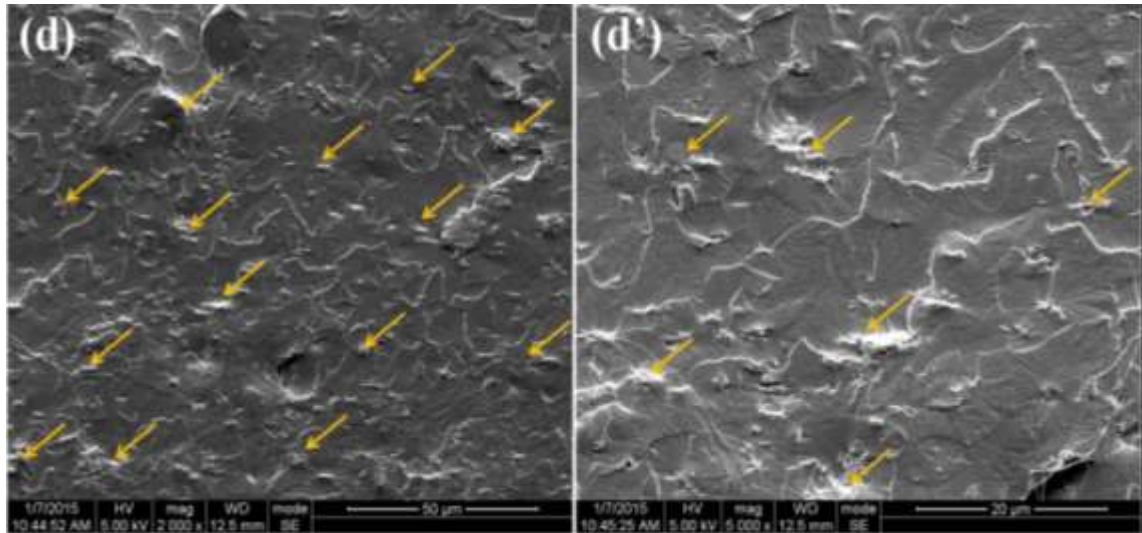


Figure S3. The SEM images of the cryo-fractured surfaces of PLGNw0.5, magnification of 2000x and 5000x (a and a'), PLGNw2.0, magnification of 2000x and 5000x (b and b'), PLGNp0.3, magnification of 2000x and 5000x (c and c'), and PLGNp1.0, magnification of 2000x and 5000x (d and d').

The dispersion of RGO subjected to bath and probe ultrasound was examined by a field-emission Scanning electron microscope (SEM) (Inspect F, FEI, Finland) with the accelerated voltage of 5 kV. The nanocomposite film prepared by compressing molding at 180 °C using the coagulated nanocomposite, was cryo-fractured in liquid nitrogen and then coated with a thin layer of gold prior to being observed.

Figure S3 exhibits the SEM images for the cryo-fractured surfaces of PLA/RGO nanocomposites, where RGO platelets are pointed out by the yellow arrows. Obviously, the aggregation can't be observed in all the systems, suggesting that regardless of the treatment method and time, the ultrasonically treated RGO is

homogeneously dispersed in the PLLA matrix. Besides, more RGO platelets are marked out with the increase of the treatment time, such as RGOw0.5 vs RGOw2.0 and RGOp0.3 vs RGOp1.0. It is mainly because the fragment of the RGO platelets caused by ultrasound dispersion.

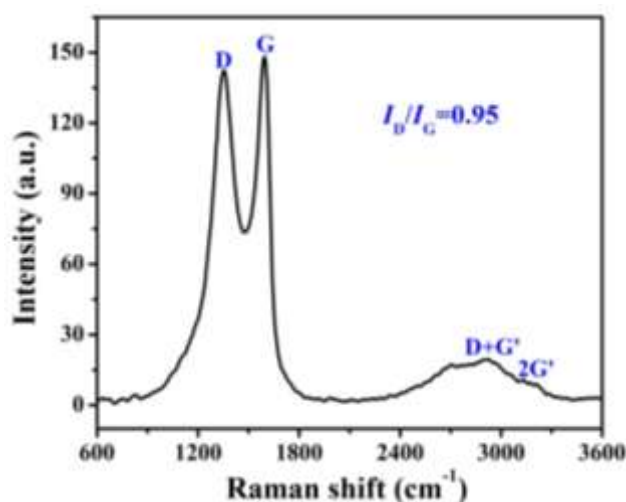


Figure S4. Raman spectra of pristine RGO for the excitation at 532 nm.

Figure S4 shows the Raman spectra of the pristine RGO. It can be seen that the I_D/I_G value of pristine RGO is 0.95, which is slightly higher than that of RGO dispersed by ultrasound treatment. It demonstrates ultrasound treatment causes the local restoration of pristine planar sp^2 carbon network. Previous study found that ethanol could repair the etch holes by facilitating the formation of new hexagonal carbon rings.³ Based on this, the higher I_D/I_G ratio could be attributed to the formation of new hexagonal carbon rings in ethanol during ultrasound treatment, which could be also evidenced from the higher C-C (C=C) content in ultrasonically treated RGO exhibited in XPS results.

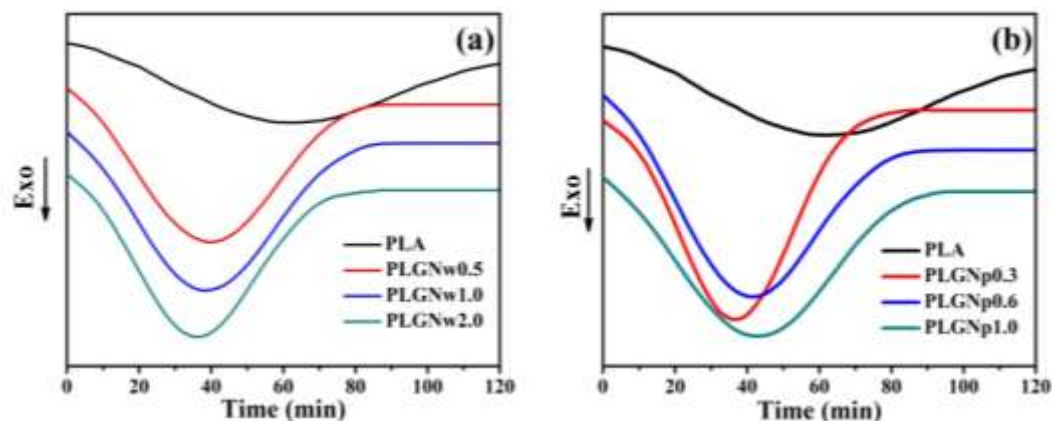


Figure S5. DSC curves of PLA and its (a) RGOw and (b) RGOp nanocomposites isothermally crystallized at 135 °C.

The crystallization kinetics of PLA and its nanocomposites was examined on a TA-Q2000 Differential Scanning Calorimetry (DSC) (TA Instruments, USA) which was performed under a nitrogen flow and calibrated by indium as the standard. For isothermal crystallization, samples were first heated to 200 °C at a rate of 30 °C/min and held for 5 min to eliminate any thermal history and then quenched at a rate of 30 °C/min to the isothermal crystallization temperature of 135 °C. The crystallization curves of PLGNw and PLGNp nanocomposites were depicted in Figure S5a and b, respectively. In comparison to neat PLA, the presence of RGO sharpened the crystallization exothermic peak of PLA matrix, suggesting the excellent nucleation ability of RGO.⁴ It was worthy to note that the accelerating effect of RGOw enhanced with the increase of ultrasound time, that was, the peak time of exothermic heat curve shifted from 41 min for PLGNw0.5 to 35 min for PLGNw2.0, while there was an opposite trend for the case in PLGNp nanocomposites. This demonstrated that nucleation efficiency of RGO featured ultrasound methods-dependence.

REFERENCES

- (1) Schniepp, H.C.; Kudin, K.N.; Li, J.L.; Prud'homme, R.K.; Car, R.; Saville, D.A.; Aksay, I.A. Bending properties of single functionalized graphene sheets probed by atomic force microscopy. *ACS Nano* **2008**, *2*, 2577-2584.
- (2) Rafiee, M. A.; Rafiee, Z.; Wang, H.; Song, Z. Z.; Yu, N. Enhanced mechanical properties of nanocomposites at low graphene content. *ACS Nano* **2009**, *3*, 3884–3890.
- (3) Gong, C.; Acik, M.; Abolfath, R. M.; Chabal, Y.; Cho, K. Graphitization of graphene oxide with ethanol during thermal reduction. *J. Phys. Chem. C* **2012**, *116*, 9969-9979.
- (4) Xu, J. Z.; Chen, T.; Yang, C. L.; Li, Z. M.; Mao, Y. M.; Zeng, B. Q.; Hsiao, B. S. Isothermal crystallization of poly(L-lactide) induced by graphene nanosheets and carbon nanotubes: A comparative study. *Macromolecules* **2010**, *43*, 5000-5008.